



# PPAR $\alpha$ activator irbesartan suppresses the proliferation of endometrial carcinoma cells via SREBP1 and ARID1A

YU LU<sup>1</sup>; TSUTOMU MIYAMOTO<sup>1,\*</sup>; HODAKA TAKEUCHI<sup>1</sup>; FUMI TSUNODA<sup>1</sup>; NAOKI TANAKA<sup>2,3,4</sup>; TANRI SHIOZAWA<sup>1</sup>

<sup>1</sup> Department of Obstetrics and Gynecology, School of Medicine, Shinshu University, Matsumoto, 390-8621, Japan

<sup>2</sup> Department of Global Medical Research Promotion, School of Medicine, Shinshu University Graduate, Matsumoto, Nagano, 390-8621, Japan

<sup>3</sup> International Relations Office, School of Medicine, Shinshu University, Matsumoto, Nagano, 390-8621, Japan

<sup>4</sup> Research Center for Social Systems, Shinshu University, Matsumoto, Nagano, 390-8621, Japan

**Key words:** Peroxisome proliferator-activated receptor alpha, Sterol regulatory element-binding protein 1, Antioxidant, Migration

**Abstract:** Endometrial carcinoma (EMC) is associated with obesity; however, the underlying mechanisms have not yet been elucidated. Peroxisome proliferator-activated receptor alpha (PPAR $\alpha$ ) is a nuclear receptor that is involved in lipid, glucose, and energy metabolism. PPAR $\alpha$  reportedly functions as a tumor suppressor through its effects on lipid metabolism; however, the involvement of PPAR $\alpha$  in the development of EMC remains unclear. The present study demonstrated that the immunohistochemical expression of nuclear PPAR $\alpha$  was lower in EMC than in normal endometrial tissues, suggesting the tumor suppressive nature of PPAR $\alpha$ . A treatment with the PPAR $\alpha$  activator, irbesartan, inhibited the EMC cell lines, Ishikawa and HEC1A, by down-regulating sterol regulatory element-binding protein 1 (SREBP1) and fatty acid synthase (FAS) and up-regulating the tumor suppressor genes p21 and p27, antioxidant enzymes, and AT-rich interaction domain 1A (ARID1A). These results indicate the potential of the activation of PPAR $\alpha$  as a novel therapeutic approach against EMC.

## Introduction

According to the statistics of the American Cancer Society, endometrial carcinoma (EMC) is one of the most important cancers among women [1], and its incidence has been increasing in recent years. The number of EMC patients has continued to increase, particularly in developed countries, which may be attributed to lifestyle changes and high-calorie diets, and obesity has been identified as one of the most critical risk factors for EMC [2]. Previous studies suggested the underlying mechanisms linking obesity and EMC, which include insulin resistance, adipokines, inflammation, and metabolic syndrome; however, a clear explanation has not yet been established.

Tumor cells are considered to undergo metabolic reprogramming in response to an augmented need for energy [3]. This reprogramming increases the production and consumption of metabolic intermediates during biosynthesis, which are regarded as a hallmark of cancer [4].

Well-known metabolic changes in tumors are the increased uptake and use of glucose, called the Warburg effect. In addition, tumor cells have been reported to show an increase in lipid synthesis in association with glucose metabolism [5]. Therefore, changes in lipid metabolism, particularly fatty acid (FA) synthesis and oxidation, are being increasingly regarded as essential events in tumor growth and aggressiveness.

Fatty acid synthase (FAS), which generates various FAs, is normally expressed in the liver, and is limited in other tissues. However, cancer tissues and normal tissues exhibiting strong proliferative activity, such as the normal endometrium, express higher levels of FAS [6], suggesting a relationship between FAS expression and proliferative potential. Sterol regulatory element-binding proteins (SREBPs) are membrane-bound transcription factors that belong to the basic helix-loop-helix leucine zipper family [7–9]. Recent studies revealed that sterol regulatory factor-binding protein-1 (SREBP1) is a key transcriptional factor involved in lipogenesis including FAS [10] because its binding elements (sterol response elements) are present in the promoter regions of genes for the biosynthesis of FAs, lipids, and cholesterol. A previous study reported that the expression of SREBP1 co-localized with that of FAS and the

\*Address correspondence to: Tsutomu Miyamoto, tmiya@shinshu-u.ac.jp

Received: 13 August 2022; Accepted: 14 March 2023;

Published: 24 May 2023



proliferation marker, Ki-67 [10]. In addition, the overexpression of SREBP1 has been detected in several cancers, such as the liver, breast, prostate, and bladder; therefore, the up-regulated expression of FAS in tumor cells is considered to be related to the overexpression of SREBP1 [11–14].

In contrast to SREBP1, peroxisome proliferator-activated receptor alpha (PPAR $\alpha$ ) is a ligand-activated, nuclear receptor/transcriptional factor that is mainly expressed in the liver, heart, kidneys, and skeletal muscle, and is involved in the activation of FA catabolism and subsequent reduction of FA/triglyceride (TG) levels by beta-oxidation [15–17]. It may also reduce the toxicity of a high cholesterol diet in the human body [18]. Although a previous study reported that fenofibrate, a PPAR $\alpha$  activator, suppressed the proliferation of and induced apoptosis in EMC cells [19], the underlying mechanisms remains unclear. The activation of PPAR $\alpha$  has been shown to suppress the LXR-SREBP1 pathway [20], indicating that PPAR $\alpha$  is a potent negative regulator of SREBP1. In addition, a PPAR $\alpha$  activator was found to reduce the nuclear expression of SREBP1 in rat liver cancer cells, and this decrease was mediated by the up-regulated expression of insulin-induced gene 1 [21], a key regulator of SREBP1. Collectively, these findings suggest that the tumor suppressor function of PPAR $\alpha$  is mediated by a reduction in the expression of SREBP1.

In addition to SREBP1, recent studies reported the involvement of cell cycle regulators in the PPAR $\alpha$ -induced growth suppression of tumor cells. p21 and p27 are important members of the cyclin-dependent kinase inhibitor family [22]. Previous findings demonstrated that a PPAR $\alpha$  activator suppressed the development of colon cancer by up-regulating the expression of p21 and p27, suggesting a PPAR strategy for the prevention of colon cancer [23]. Moreover, an abnormality in the AT-rich interaction domain 1A (ARID1A) gene, an essential molecule in chromosomal stability, was shown to be closely involved in the development of EMC [24]; however, the role of ARID1A in PPAR $\alpha$ -mediated growth regulation has not been examined.

Irbesartan (Irbe), a conventional angiotensin II receptor blocker, is frequently used as an antihypertensive drug in clinical practice. In contrast to fibrates, Irbe activates PPAR $\alpha$  without significant adverse effects [25]. Hypertension is an important risk factor for EMC [2], and angiotensin II has been reported to promote the survival of EMC cells [26]. In addition, the activation of PPAR $\alpha$  by fibrates was previously shown to inhibit the growth of EMC cells *in vitro* via PPAR $\alpha$  [19]. Therefore, Irbe has potential as a therapeutic agent for EMC.

Accordingly, we hypothesized that the effects of PPAR $\alpha$  on tumor cells may be attributed to abnormal lipid metabolism and the related expression of tumor suppressors. To test this hypothesis, we investigated the expression and function of PPAR $\alpha$  by immunohistochemistry, gene silencing, and with the PPAR $\alpha$  activator, Irbe, using EMC Ishikawa cells. In addition, the involvement of SREBP1, p21 and p27, and ARID1A was examined using immunoblotting and immunofluorescence.

## Materials and Methods

### Immunohistochemistry

#### 1) Collection of normal and neoplastic endometrial tissues

Formalin-fixed, paraffin-embedded tissues of the normal endometrium (5 cases each of the proliferative and secretory phases) and EMC (22 cases of Grade 1 (G1), 14 of Grade 2 (G2), and 14 of Grade 3 (G3)) were collected from the pathology files of patients who underwent biopsy or hysterectomy at Shinshu University Hospital in Matsumoto City between 2020 and 2021. All participants were Japanese individuals living in Nagano prefecture, Japan. The median age of participants with a normal endometrium was 46 years (35 to 49 years, premenopausal), while that of EMC patients was 55 years (29 to 83 years). These EMC patients included 24 cases (12 in G1, 5 in G2, and 7 in G3) with a body mass index (BMI) >25, defined as obese in Japan. We used tissue sections from these patients for immunohistochemical and hematoxylin and eosin (HE) staining.

#### 2) Staining procedure

We performed immunohistochemical staining as previously described [27]. Briefly, indirect immunostaining for PPAR $\alpha$ , SREBP1, and FAS was conducted using anti-PPAR $\alpha$  (1:100 dilution, mouse monoclonal, H-2, sc-398394, Santa Cruz Biotechnology, Dallas, TX, USA), anti-SREBP1 (1:100 dilution, rabbit polyclonal, NB100-2215, Novus Biologicals, Centennial, CO, USA), and anti-FAS (1:500 dilution, rabbit monoclonal, C18C12, #4233, Cell Signaling Technology, Danvers, MA, USA) antibodies, respectively, as primary antibodies. N-Histofine<sup>®</sup> Simple Stain Max-PO(M) and (R) (414132F and 414142F, Nichirei Biosciences Inc., Tokyo, Japan) were used as the secondary antibodies for anti-PPAR $\alpha$  and anti-SREBP1, respectively. Three-micrometer-thick sections were deparaffinized in d-Limonene (Hemo-De<sup>®</sup>, FALMA, Tokyo, Japan) and rehydrated in a graded alcohol series. Antigens were retrieved by a microwave pretreatment in 10 mM Tris/HCl buffer (pH 8.0) containing 1 mM EDTA for 30 min. Sections were then exposed to primary antibodies at 4°C overnight. As a positive control, we used kidney tissue sections for anti-PPAR $\alpha$  and anti-SREBP1 antibodies and breast cancer tissue sections for anti-FAS antibodies (Suppl. Fig. S1). As a negative control, tissue sections were treated with a buffered solution without the primary antibody. These sections were then incubated with the secondary antibody at room temperature for 60 min. The immunocomplex was visualized by diaminobenzidine (349-00903, FUJIFILM Wako Pure Chemical, Osaka, Japan).

#### 3) Staining evaluation

The immunoreactivity of each stain was assessed by the Histo Score (H-score). We took three microscopic photographs per immunostaining slide at  $\times 200$  magnification and automatically counted nuclei with each nuclear staining intensity (strong, moderate, weak, and no stain) using free ImageJ software (<https://imagej.nih.gov/ij/>). Nuclear staining intensity was graded as follows: 0 = no stain (similar to the negative control), 1 = weak stain, 2 =

moderate stain (equivalent to the positive control), and 3 = strong stain. The H-score was calculated using the following formula:  $[1 \times (\% \text{ nuclei with weak staining}) + 2 \times (\% \text{ nuclei with moderate staining}) + 3 \times (\% \text{ nuclei with strong staining})]$ . The final score ranged between 0 and 300. Cytoplasmic staining for FAS was also automatically counted using ImageJ and evaluated by the H-score.

#### Cell culture

EMC cells: The ER $\alpha$ -positive EMC cell line, Ishikawa 3-H-12 (Ishikawa), was kindly gifted from Dr. Nishida (Kasumigaura Medical Center, Tsuchiura, Japan) through the Japanese Collection of Research Bioresources (JCRB) Cell Bank (JCRB1505, Ibaraki, Japan). The ER $\alpha$ -negative EMC cell line, HEC1A, was purchased from the American Type Culture Collection (HTB-112, Manassas, VA, USA). Among the EMC cell lines we had, these two showed high PPAR $\alpha$  expression (Suppl. Fig. S2). Ishikawa cells were cultured in Dulbecco's modified Eagle medium (D6046, Sigma-Aldrich, St. Louis, MO, USA) supplemented with 15% fetal bovine serum (FBS) (10270-106, Thermo Fisher Scientific, Waltham, MA, USA). HEC1A cells were cultured in McCoy's 5A medium (M9309, Sigma-Aldrich) supplemented with 10% FBS. Cells were incubated at 37°C in a 5% CO $_2$  incubator.

#### siRNA transfection

Ishikawa and HEC1A cells were transfected with siRNA as previously described [28]. In brief, on the day before use in experiments, cells were seeded on 6-well plates at a density of  $2 \times 10^5$  cells/well. After 24 h, cells in the siPPAR $\alpha$  group were treated with 5 nM siRNA for PPAR $\alpha$  (CCUUGCAGGCCACUCGAGCCCUAAU) (Stealth RNAi<sup>TM</sup> siRNA, Thermo Fisher Scientific). Lipofectamine RNAiMAX Reagent (Cat. No. 13778030, Thermo Fisher Scientific) was used for siRNA transfection according to the manufacturer's instructions. The negative control (NC) group received Stealth RNAi<sup>TM</sup> siRNA negative control lo GC (12935-200, Thermo Fisher Scientific). Cells were then used in subsequent experiments. After transfection for 72 h, cells were harvested to confirm silencing by Western blotting and RT-PCR.

#### Agents

Irbe, used in experiments as an inducer of PPAR $\alpha$  expression, was purchased from Sigma-Aldrich (Cas No. 138402-11-6) and dissolved in dimethyl sulfoxide (DMSO) (FUJIFILM Wako Pure Chemical) for addition to cultured cells. Cells in the Irbe group were treated with 100  $\mu$ M Irbe. This concentration was selected based on previous studies [25,29]. Cells in the NC group were treated with DMSO only.

#### Cell proliferation assay

The WST-1 assay was performed to examine the effects of PPAR $\alpha$  on cell proliferation using Cell Proliferation Reagent WST-1 (Code: 11644807001, Roche Diagnostics, Basel, Switzerland) and a microplate reader (BioTek Synergy HTX Multimode Reader: Agilent Technologies, Santa Clara, CA, Japan). As previously described [28], cells were seeded on a 96-well microplate at a density of 1000 cells/well. According to the manufacturer's instructions, the WST-1 assay was

performed for 4 consecutive days after the confirmation of cell attachment to the bottom of the wells. All experiments were conducted using eight wells for each condition and repeated three or more times to confirm reproducibility.

#### Scratch wound healing assay

The effects of PPAR $\alpha$  on migration were analyzed by the scratch wound healing assay using Ishikawa and HEC1A cells and then compared between PPAR $\alpha$  siRNA (siPPAR $\alpha$ ) and NC siRNA (NC) or between Irbe and DMSO (NC). Cells were prepared as previously described [30]. In brief,  $8.2 \times 10^4$  cells were plated onto 6-well plates and cultured under each condition, such as siRNA transfection or the Irbe treatment. The surface of the plates containing cells at 70% confluence was scratched linearly with a new 200- $\mu$ l pipette tip to form the gap recorded by photographs (0 h,  $\times 200$  magnification by phase contrast observations). After 48 h, we photographed the same gap positions (48 h). ImageJ software automatically measured the area occupied by migrated cells in the gap formed by the scratch at 48 h in these photographs. We obtained results from 3 independent experiments with three or more measurement points.

#### Western blotting

Protein expression levels in Ishikawa and HEC1A cells were examined by Western blotting, as previously described [28]. In brief,  $8.2 \times 10^4$  EMC cells were cultured in a 6-well plate. Cells were harvested 72 h after gene silencing and drug treatment and lysed in 100  $\mu$ L of lysis buffer. The supernatant protein was extracted by  $-80^\circ\text{C}$  quick freezing and thawing on ice. Protein concentrations were measured using the Pierce<sup>TM</sup> BCA Protein Assay kit (Cat: 23227, Thermo Fisher Scientific). The nuclear and cytoplasmic fractions of cell extracts were prepared using NE-PER<sup>TM</sup> Nuclear and Cytoplasmic Extraction Reagent (Thermo Fisher Scientific). Immunoblotting was performed using antibodies targeting PPAR $\alpha$  (1:200, sc-398394), SREBP1 (1:100, NB100-2215), FAS (1:1000, C18C12, #4233), the cell cycle-dependent kinase inhibitors p21 (1:500, mouse monoclonal, Cat. No: 554228, BD Pharmingen, San Diego, CA, USA) and p27 (1:200, mouse monoclonal, sc-1641, Santa Cruz Biotechnology), superoxide dismutase 1 (SOD1, 1:5000, mouse monoclonal, sc-17767, Santa Cruz Biotechnology) superoxide dismutase 2 (SOD2, 1:1000, rabbit monoclonal, D9V9C, #13194, Cell Signaling Technology), glutathione peroxidase 1 (GPx1, 1:200, mouse monoclonal, sc-22146, Santa Cruz Biotechnology), NADH quinone oxidoreductase (NQO1, 1:1000, rabbit polyclonal, Cat. No. GTX100235, GeneTex, Irvine, CA, USA), and ARID1A (1:1000, rabbit polyclonal, HPA005456, Sigma-Aldrich). The bands of  $\beta$ -actin (1:1000, mouse monoclonal, A5441, Sigma-Aldrich) and Lamin B1 (1:2000, mouse monoclonal, NA-12-100UG, Oncogene, Boston, MA, USA) were used as the loading controls of whole-cell lysates and nuclear fractions, respectively. Protein-transferred membranes were incubated with the specific primary antibody at 4°C overnight and then with the secondary antibody at room temperature for 1 h. The target protein band bound by the antibody complex was then visualized using the ECL Western blot detection reagent (RPN-2109, Amersham, Amersham, UK). Image J software

was used to analyze band density. Band densities were calculated relative to the density of  $\beta$ -actin and Lamin B1 expression. All experiments were repeated three or more times to confirm reproducibility.

#### Real-time quantitative RT-PCR (qPCR) analysis

The expression of mRNA in Ishikawa cells was analyzed by real-time qPCR. The total RNA of cells cultured on 6-well plates under specific conditions was isolated using TRIzol reagent (Cat. No. 15596026, Thermo Fisher Scientific). Reverse transcription (RT) and qPCR were performed using the PrimeScript RT-PCR kit (RR014B, Takara Bio, Shiga, Japan) according to the manufacturer's instructions. Primer sequences are listed in [Suppl. Table S1](#). The mRNA expression levels of each gene were corrected by the mRNA expression level of ACTB, the endogenous control, and shown as a relative value to NC. Experiments were repeated three times with four replicates.

#### Reactive oxygen species (ROS) assay

We investigated the effects of the Irbe treatment on intracellular ROS production in Ishikawa cells. A total of  $5 \times 10^3$  cells/well of Ishikawa cells were plated on 96-well plates. After cells had attached to the bottom of the well, they were treated with 100  $\mu$ M Irbe (the Irbe group) or DMSO only (the NC group) for 24 h. Intracellular ROS production was measured using a Fluorometric Intracellular ROS Kit (MAK143, Sigma-Aldrich) according to the manufacturer's instructions. Experiments were repeated three times with eight replicates.

#### Immunofluorescent staining analysis

We performed dual immunofluorescent staining for PPAR $\alpha$  and SREBP1, p21, or p27 in Irbe-treated (Irbe group) and DMSO-treated (NC group) Ishikawa cells, as previously described [31]. We used a mouse monoclonal anti-PPAR $\alpha$  antibody (working concentration 4  $\mu$ g/mL, sc-398394, Santa Cruz Biotechnology) and Alexa Fluor<sup>®</sup> 594-conjugated goat anti-mouse IgG antibody (red-fluorescence, A-11005, Thermo Fisher Scientific) for PPAR $\alpha$ . We used rabbit polyclonal primary antibodies (anti-SREBP1: working concentration 4  $\mu$ g/mL, NB100-2215, Novus Biologicals; anti-p21: working concentration 0.2  $\mu$ g/mL, sc-756, Santa Cruz Biotechnology; anti-p27: working concentration 0.2  $\mu$ g/mL, sc-528, Santa Cruz Biotechnology) and an Alexa Fluor<sup>®</sup> 488-conjugated goat anti-rabbit IgG antibody (green-fluorescence, A-11008, Thermo Fisher Scientific) for SREBP1, p21, and p27.

A total of  $2 \times 10^4$  Ishikawa cells/well were cultured in 8-well chamber slides and treated for 24 h. Cells were washed once with phosphate-buffered saline (PBS) and then fixed with 4% paraformaldehyde phosphate buffer (09154-56, Nacalai Tesque, Kyoto, Japan) for 15 min. After washing with PBS, cells were blocked with 1% bovine serum albumin (Sigma-Aldrich) in PBS for one hour at room temperature, the primary antibody was added, and cells were then incubated at 4°C overnight. After washing with PBS, cells on slides were covered with the secondary antibody solution and set in the dark for one hour. After washing with PBS, cells were nuclear-counterstained by DAPI (D9542, Sigma-

Aldrich) and sealed with Fluorescence Mounting Medium (S3023, DAKO, Glostrup, Denmark). All specimens were observed at  $\times 200$  magnification using the Zeiss LSM880 confocal imaging system (Carl Zeiss, Oberkochen, Germany). We used ImageJ software to measure the immunofluorescent signal intensity of photographs. Experiments were repeated three times.

#### Statistical analysis

All data are presented as the mean  $\pm$  standard deviation. The results of immunostaining of the endometrium were evaluated using Scheffé's method, and other comparisons of two groups were conducted using the Student's *t*-test.  $p < 0.05$  was considered to be significant.

## Results

### PPAR $\alpha$ expression decreased, while SREBP1 and FAS expression reciprocally increased in EMC tissues

Since PPAR $\alpha$  is a nuclear receptor, we considered the nuclear staining of PPAR $\alpha$  to be significant in the normal endometrium ([Figs. 1A and 1B](#)). The H-scores of nuclear PPAR $\alpha$  expression in endometrium epithelia were  $231 \pm 26$  (mean  $\pm$  SD) in the proliferative phase and  $226 \pm 25$  in the secretory phase, with no significant difference. The H-scores of nuclear PPAR $\alpha$  expression in G1, G2, and G3 tumors were  $56 \pm 26$ ,  $51 \pm 20$ , and  $39 \pm 19$ , respectively, with a significant difference between G1 and G3. However, the H-score of nuclear PPAR $\alpha$  was significantly lower in all EMC tumors than in normal endometrium epithelia ( $p < 0.01$ ). SREBP1 is an inactive precursor that binds to the endoplasmic reticulum. It is transported from the endoplasmic reticulum to the Golgi apparatus, in which it is activated. Activated SREBP1 is then transferred to the nucleus to synthesize cholesterol and FAs [8, 32, 33]. The H-scores of nuclear SREBP1 expression in the proliferative and secretory phases of endometrium epithelia were  $11 \pm 7$  and  $12 \pm 9$ , respectively, with no significant difference ([Figs. 1A and 1C](#)). The H-scores of nuclear SREBP1 expression in G1, G2, and G3 tumors were  $83 \pm 34$ ,  $86 \pm 34$ , and  $100 \pm 20$ , respectively, with no significant differences ([Figs. 1A and 1C](#)).

However, the H-score of nuclear SREBP1 was significantly higher in all EMC tumors than in the normal endometrium ( $p < 0.01$ ). Similar to SREBP1, the H-score of cytoplasmic FAS was significantly higher in EMC than in normal endometrial epithelia ( $p < 0.01$ ) ([Figs. 1A and 1D](#)). These results indicate that as PPAR $\alpha$  expression decreased, SREBP1 and FAS reciprocally increased in EMC.

In this EMC case series, we compared the expression of PPAR $\alpha$ , SREBP1, and FAS between obese Japanese patients with BMI  $> 25$  ( $n = 24$ ) and non-obese patients with BMI  $< 25$  ( $n = 26$ ), but observed no significant difference ([Fig. 1E](#)). However, a weak correlation was noted between BMI and the H-scores of PPAR $\alpha$  (inverse correlation), SREBP1, and FAS by Spearman's rank correlation ([Fig. 1F](#)).

### PPAR $\alpha$ suppresses the proliferation and migration of EMC cells

To investigate the effects of PPAR $\alpha$  on the growth of EMC cells, we examined the effects of PPAR $\alpha$  silencing using the

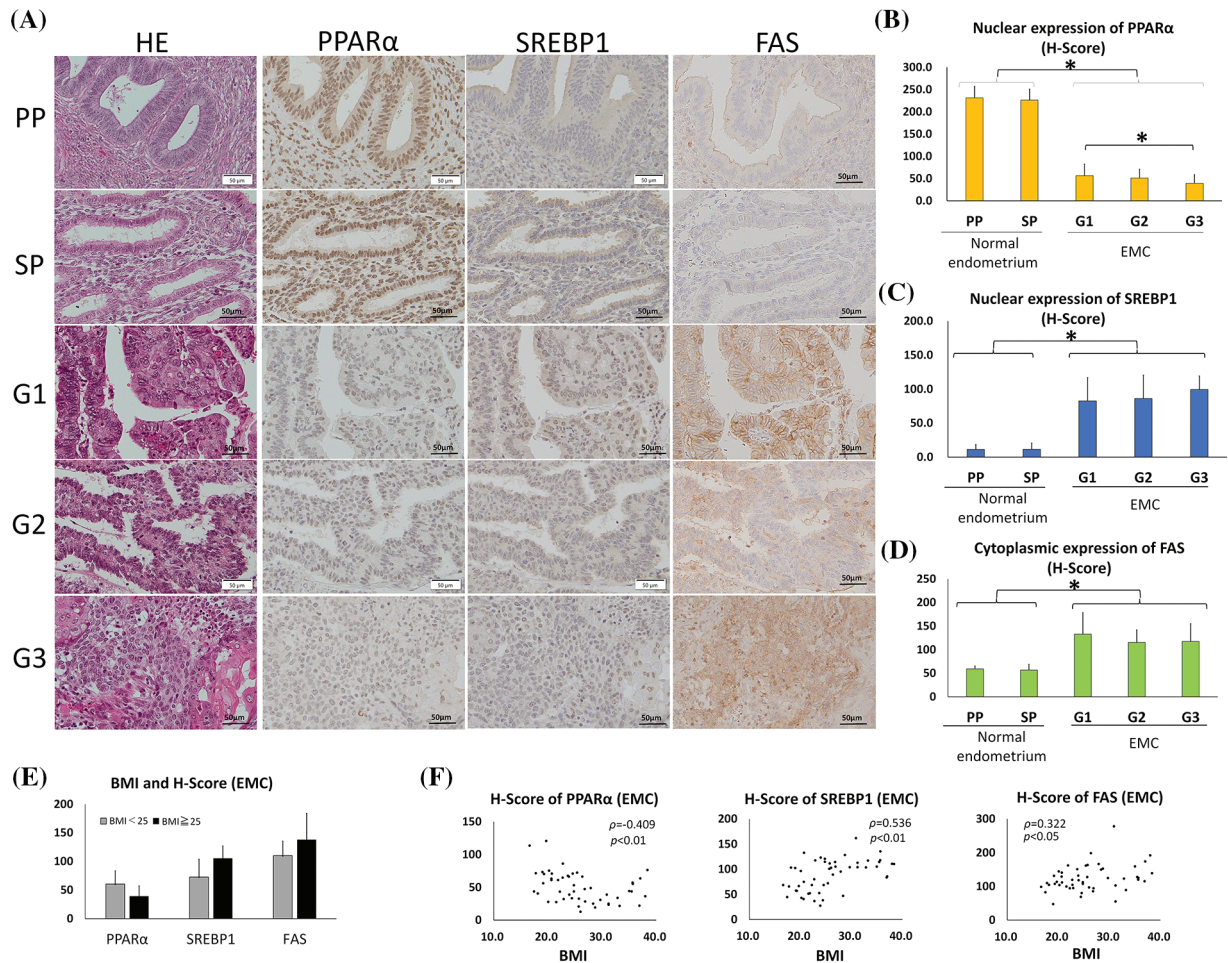


**FIGURE 1.** PPAR $\alpha$  expression was lower and SREBP1 and FAS expression was higher in endometrial carcinoma (EMC) than in normal endometrial glands. (Immunohistochemistry). (A) Photomicrographs show hematoxylin and eosin (HE) staining and representative immunostaining for PPAR $\alpha$ , SREBP1, and FAS in serial sections of the normal endometrium (PP: proliferation phase; SP: secretory phase) and EMC (G1: grade 1; G2: grade 2; G3: grade 3). (B–D) Graphic demonstration of immunostaining for PPAR $\alpha$  (B), SREBP1 (C), and FAS (D). The expression of PPAR $\alpha$  was significantly lower in EMC than in the normal endometrium, while the expression of SREBP1 and FAS was significantly higher ( $* p < 0.01$ ). (E) The graph indicates the H-scores of PPAR $\alpha$ , SREBP1, and FAS in non-obese EMC patients with BMI <25 ( $n = 26$ ) or in obese EMC patients with BMI  $\geq$ 25 ( $n = 24$ ). There was no significant difference. (F) The BMI and H-scores of PPAR $\alpha$ , SREBP1, and FAS in each EMC patient are shown in scatter plots. Spearman's rank correlation coefficient showed a weak inverse correlation between BMI and the PPAR $\alpha$  H-score and a moderate or weak correlation between BMI and SREBP1 or FAS.

EMC cell lines, Ishikawa and HEC1A. We found that PPAR $\alpha$  silencing significantly increased the proliferation of both cell lines at 72 h (Fig. 2A). The addition of Irbe significantly suppressed the growth of Ishikawa and HEC1A cells at 72 h (Fig. 2B). The growth suppressive effects of Irbe (siControl + Irbe, Fig. 2C) relative to untreated NC cells (siControl + DMSO) were almost fully canceled by PPAR $\alpha$  silencing (siPPAR $\alpha$  + Irbe) in both EMC cell lines (Fig. 2C). Therefore, we considered Irbe to exert anti-proliferative effects by activating PPAR $\alpha$ . Immunoblotting results also showed that the Irbe treatment (siControl + Irbe) up-regulated the protein expression of PPAR $\alpha$  and down-regulated that of SREBP1 (Fig. 2D). This effect of Irbe was canceled by the inhibition of PPAR $\alpha$  expression (siPPAR $\alpha$  + Irbe, Fig. 2D). These results demonstrated that Irbe suppressed the proliferation of EMC cells by up-regulating PPAR $\alpha$  expression.

The effects of PPAR $\alpha$  on cell migration were examined using the scratch wound healing assay. In comparisons with

the NC, migration activity increased after the PPAR $\alpha$  gene was silenced (Fig. 2E), and the Irbe treatment up-regulated PPAR $\alpha$  expression and significantly decreased migration (Fig. 2F). These results indicate that the activation of PPAR $\alpha$  suppressed the proliferation and migration of EMC cells. In the experiments shown in Fig. 2, HEC1A and Ishikawa cells exhibited similar changes in PPAR $\alpha$  and SREBP1 protein expression and cellular functions, such as proliferative and migratory abilities, in response to PPAR $\alpha$  silencing and the Irbe treatment. Therefore, we used Ishikawa cells in subsequent experiments.

#### PPAR $\alpha$ suppresses SREBP1 and FAS expression and enhances p21 and p27 expression

The effects of PPAR $\alpha$  on the expression of SREBP1, FAS, and p21/p27 in Ishikawa cells was investigated by gene silencing and the Irbe treatment. The expression of SREBP1 and FAS was increased by PPAR $\alpha$  silencing and decreased by the

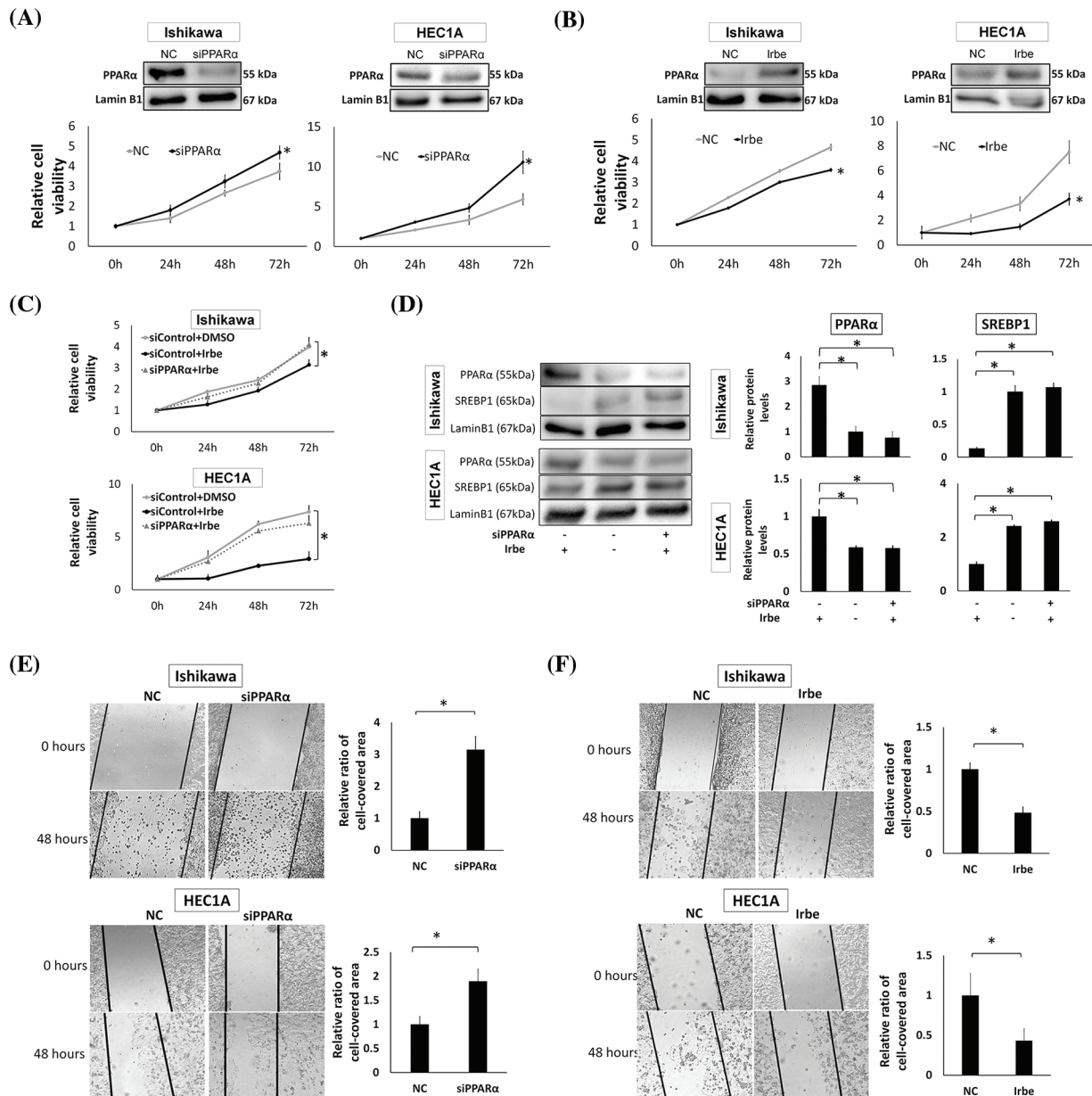


**FIGURE 2.** PPAR $\alpha$  reduces the proliferation and migration of EMC cell lines, Ishikawa and HEC1A. (A) PPAR $\alpha$  suppression by siRNA enhanced the proliferation of Ishikawa and HEC1A cells. Western blotting shows that PPAR $\alpha$  protein expression was significantly lower than that in the negative control (NC) after the treatment with PPAR $\alpha$  siRNA (siPPAR $\alpha$ ) ( $p < 0.05$ ). The WST-1 assay indicates that siPPAR $\alpha$  induced significant increases in proliferation at 72 h (h). (B) Western blotting and the WST-1 assay show that PPAR $\alpha$  protein expression was significantly higher ( $p < 0.05$ ), while Ishikawa and HEC1A cell proliferation was lower with the addition of Irbesartan (Irbe) (100  $\mu$ M) than with the NC at 72 h. (C) The Irbesartan (Irbe) treatment suppressed the proliferation of Ishikawa and HEC1A cells by up-regulating the expression of PPAR $\alpha$ . Viability was lower in cells treated with the Irbe treatment (siControl+Irbe) than in the untreated negative control (siControl+DMSO) at 72 h. However, this effect of Irbe was almost entirely canceled by the suppression of PPAR $\alpha$  by siRNA (siPPAR $\alpha$ +Irbe). (D) Western blotting showed that PPAR $\alpha$  expression was higher and SREBP1 expression was lower in both EMC cells after the Irbe treatment than in the untreated control. This effect of Irbe was canceled by the suppression of PPAR $\alpha$  by siRNA (siPPAR $\alpha$ ). (E) In comparisons with the NC, the scratch wound healing assay indicated that PPAR $\alpha$  silencing by siRNA (siPPAR $\alpha$ ) significantly facilitated the migration of Ishikawa and HEC1A cells. (F) The scratch assay also showed that the Irbe treatment (Irbe) reduced migration. \*  $p < 0.05$ .

addition of Irbe, indicating an inverse correlation between the expression of PPAR $\alpha$  and SREBP1/FAS proteins (Figs. 3A and 3B). The expression of the p21 and p27 proteins was decreased by PPAR $\alpha$  silencing and increased by the Irbe treatment, indicating a positive correlation between the expression of PPAR $\alpha$  and p21/p27 (Figs. 3C and 3D).

The mRNA expression levels of these genes were also examined using real-time qPCR. Expression levels compared with the NC are shown in Fig. 3E. Although fold changes in SREBP1 mRNA expression from that in the NC were small, the results obtained suggested that SREBP1 and FAS mRNA expression may both inversely correlate with PPAR $\alpha$  mRNA

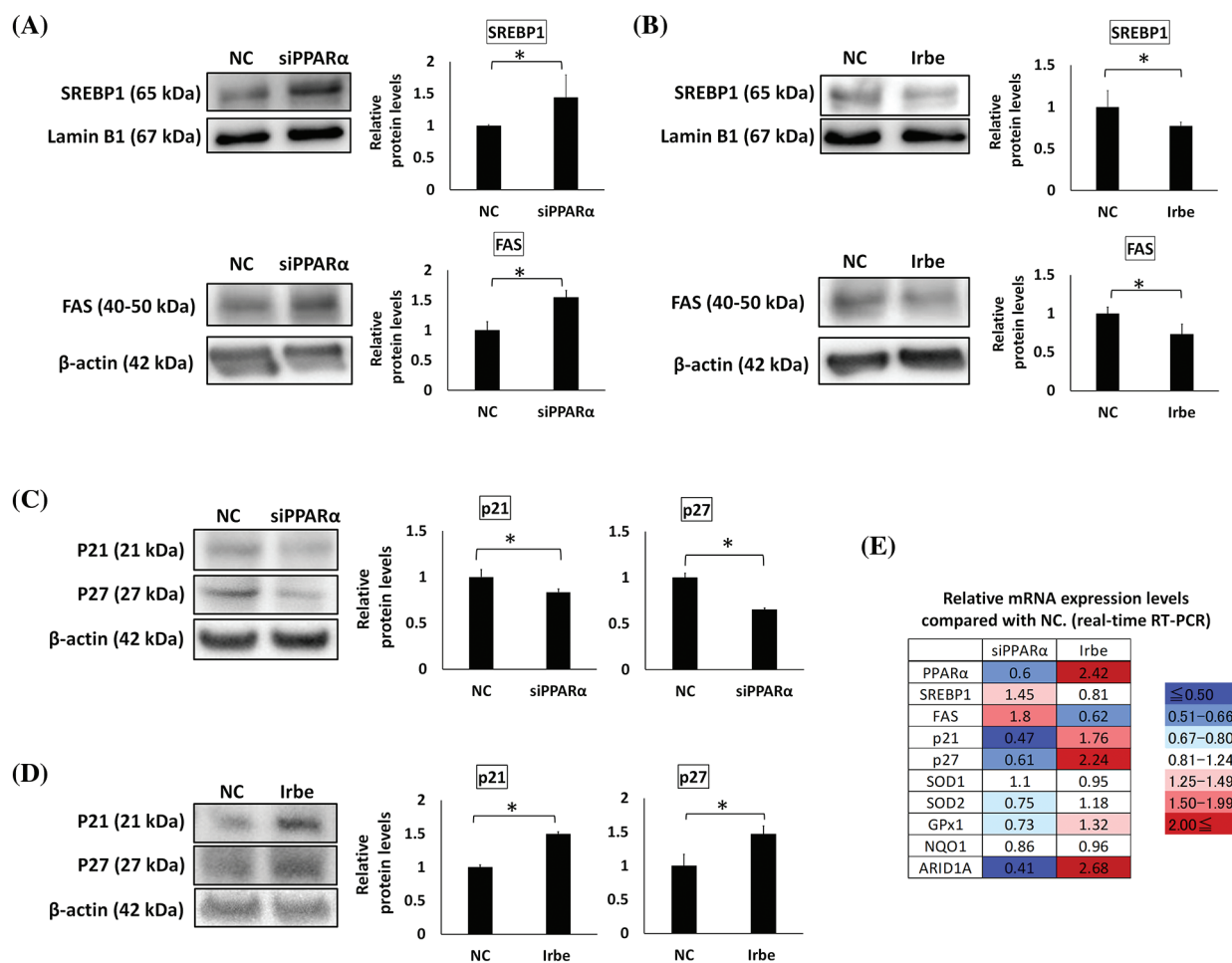


**FIGURE 3.** PPAR $\alpha$  suppresses SREBP1 and FAS expression and promotes p21 and p27 expression. (A–D) Western blotting. (E) Real-time RT-qPCR. (A) PPAR $\alpha$  gene silencing (siPPAR $\alpha$ ) increased SREBP1 and FAS protein expression over that in the negative control (NC). (B) The PPAR $\alpha$  inducer, Irbe (100  $\mu$ M) reduced SREBP1 and FAS protein expression to lower than that in the NC. (C) PPAR $\alpha$  gene silencing suppressed p21 and p27 protein expression. (D) The Irbe (100  $\mu$ M) treatment increased p21 and p27 protein expression. (E) The mRNA expression level of each gene after PPAR $\alpha$  silencing (siPPAR $\alpha$ ) and the Irbe treatment (Irbe) was measured by real-time RT-qPCR and shown as a relative value to NC. The heat map shows expression reductions in blue and expression increases in red. Although the fold change in SREBP1 was smaller than that in FAS, SREBP1 and FAS mRNA expression inversely correlated with PPAR $\alpha$ . On the other hand, the mRNA expression of p21, p27, SOD1, and GPx1 correlated with PPAR $\alpha$ . NC: negative control. \*  $p < 0.05$ .

expression, similar to protein expression. Changes in p21 and p27 expression levels also correlated with those in PPAR $\alpha$  expression levels, similar to protein expression (Fig. 3E).

#### PPAR $\alpha$ promotes antioxidant functions and ARID1A expression in EMC cells

Oxidative stress is an important factor in the formation and development of cancer [34]. Since previous studies demonstrated that PPAR $\alpha$  exerts antioxidant effects [35], we examined the effects of PPAR $\alpha$  silencing and the addition of Irbe on the expression of the typical antioxidant enzymes, SOD1, SOD2, GPx1, and NQO1, in Ishikawa cells. Real-time RT-qPCR suggested that the mRNA expression of SOD2 and GPx1 correlated with that of PPAR $\alpha$  (Fig. 3E). These results indicated that PPAR $\alpha$  silencing reduced SOD2 and GPx1 protein expression (Fig. 4A). In contrast, the Irbe treatment increased SOD2 and GPx1 protein expression (Fig. 4B). In addition, the results of the ROS assay suggested that the Irbe treatment attenuated intracellular ROS

production in Ishikawa cells (Fig. 4C). Therefore, PPAR $\alpha$  may ameliorate oxidative stress in EMC Ishikawa cells.

Since ARID1A is regarded as an important tumor suppressor in EMC, the effects of PPAR $\alpha$  silencing and activation on the expression of ARID1A were examined. The results obtained indicated that PPAR $\alpha$  silencing reduced, while the addition of Irbe increased ARID1A protein expression (Fig. 4D). These results suggest the involvement of PPAR $\alpha$  in ARID1A-mediated oncogenic suppression in endometrial cancer cells.

#### The PPAR $\alpha$ activator, Irbe, reduces SREBP1 and increases p21/p27 in PPAR $\alpha$ -activated cells

To examine changes in the subcellular distribution of PPAR $\alpha$ , SREBP1, and p21/p27 proteins in Ishikawa cells treated with Irbe, immunofluorescent staining was performed. The PPAR $\alpha$  signal was observed in nuclei, and the number of PPAR $\alpha$ -positive cells was higher after the administration of Irbe than in the NC group (Figs. 5A–5C).

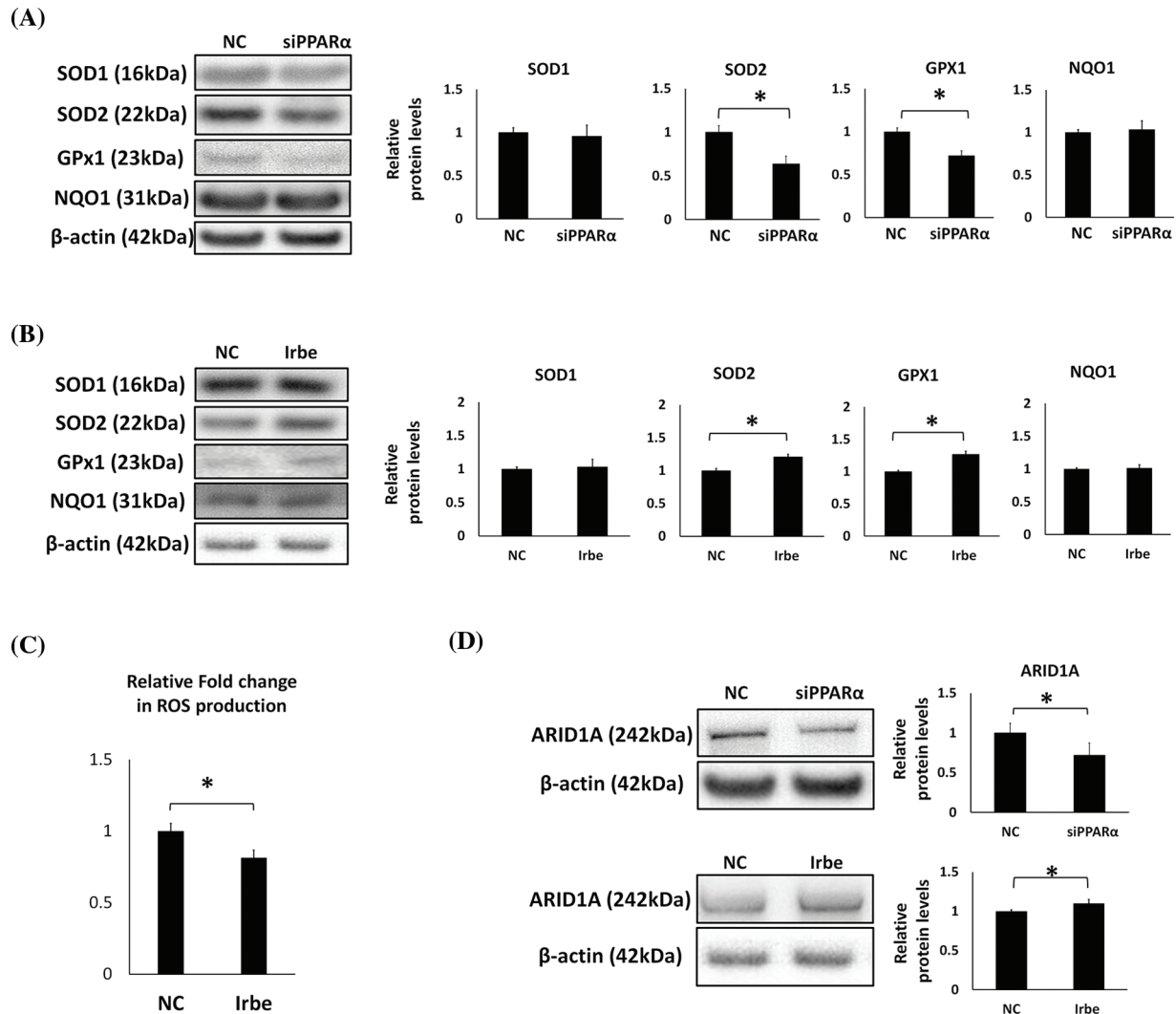


**FIGURE 4.** PPAR $\alpha$  promotes the expression of antioxidant enzymes, SOD2 and GPx1, and the vital tumor suppressor factor, ARID1A, in Ishikawa cells. (A) PPAR $\alpha$  gene silencing decreased SOD2 and GPx1 protein expression. (B) The Irbe (100  $\mu$ M) treatment increased SOD2 and GPx1 protein expression. (C) The graph shows intracellular reactive oxygen species (ROS) production measured by the ROS assay in Ishikawa cells treated with 100  $\mu$ M Irbesartan (Irbe) for 24 h or DMSO (NC). This result indicates that Irbe reduced intracellular ROS production in EMC cells. (D) PPAR $\alpha$  gene silencing decreased, while the Irbe (100  $\mu$ M) treatment increased ARID1A protein expression. \*  $p < 0.05$ .

In contrast, SREBP1-positive cells in the nucleus decreased in the Irbe-treated group (Fig. 5A). On the other hand, the Irbe treatment increased the expression of p21 and p27 (Figs. 5B and 5C). Furthermore, the distribution of PPAR $\alpha$ -positive and p21/p27-positive cells was similar to that in the Irbe group (Figs. 5B and 5C). These results were consistent with those of immunoblotting. Since activated PPAR $\alpha$  is stabilized in nuclei and enhances the transcriptional activity of target genes, increases in PPAR $\alpha$ -positive cells in nuclei indicate the sufficient activation of PPAR $\alpha$  by the Irbe treatment.

## Discussion

EMC is strongly associated with obesity; however, the underlying mechanisms remain unclear. In the present study, we demonstrated that the expression of PPAR $\alpha$ , a pivotal transcription factor for lipid metabolism, was lower in the nuclei of EMC cells than in normal endometrial cells.

In EMC tissues, the expression of PPAR $\alpha$  inversely correlates with BMI, while that of SREBP1 and its target gene, FAS, positively correlates with BMI. Although these correlations are weak, these proteins have been implicated in the development of obesity-associated EMC. Furthermore, the function of PPAR $\alpha$  was evoked via the down-regulation of SREBP1 and FAS. Irbe also significantly suppressed the proliferation of EMC cells through the activation of PPAR $\alpha$ . These results indicate that PPAR $\alpha$  functions as a tumor suppressor, and, thus, a PPAR $\alpha$  activator may be a novel promising therapeutic agent against EMC.

The present study showed that the immunohistochemical expression of PPAR $\alpha$  in normal endometrial glands was similar between the proliferative and secretory phases, suggesting that PPAR $\alpha$  expression is independent of estrogen and progesterone. In normal human tissues, PPAR $\alpha$  is abundantly expressed in the liver, heart, kidneys, and skeletal muscle. Detectable PPAR $\alpha$  was

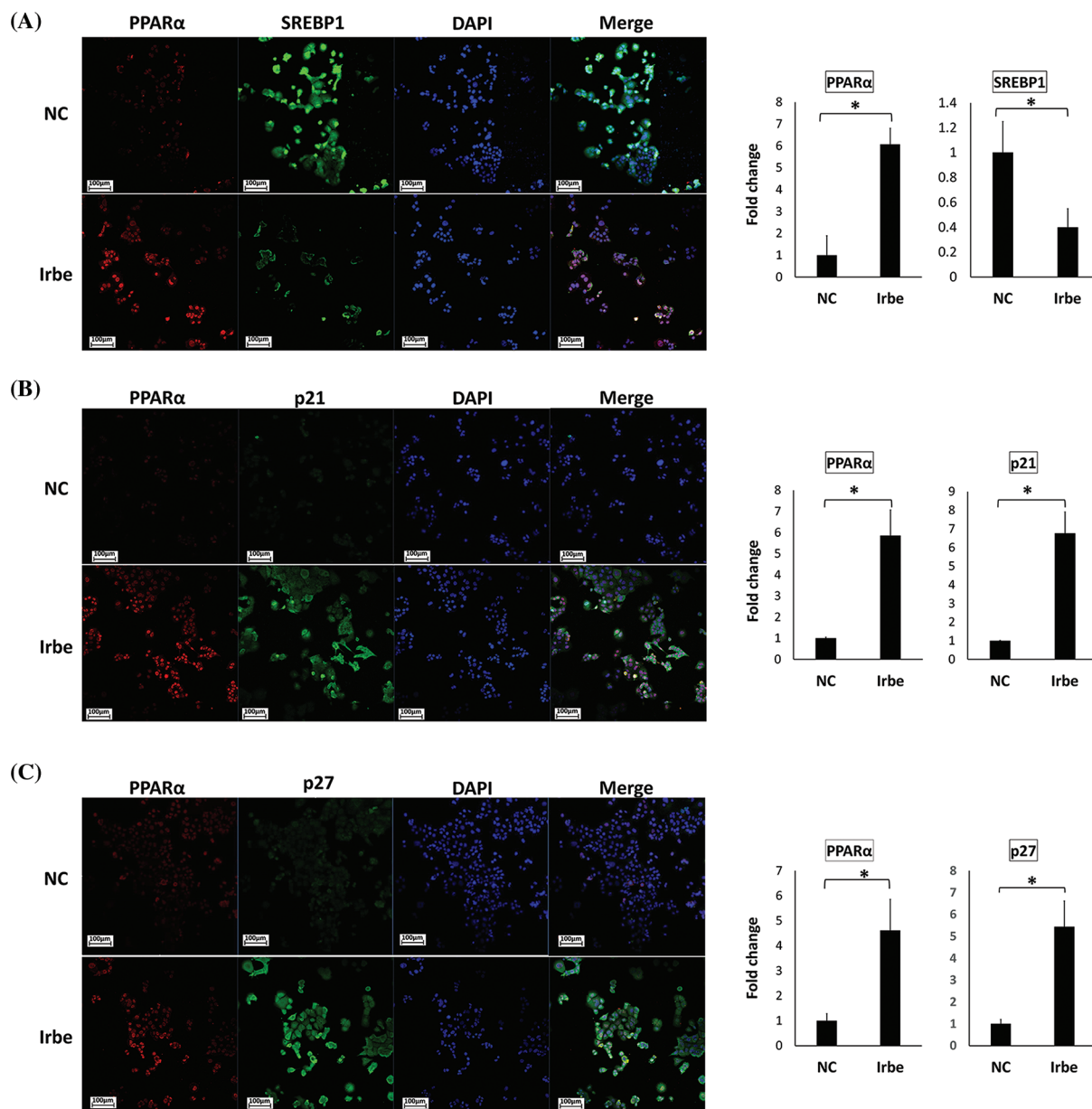


**FIGURE 5.** The PPAR $\alpha$  activator, Irbe, reduces SREBP1 expression and induces the expression and co-localization of PPAR $\alpha$  and p21/p27 in Ishikawa cells. (A) Dual immunofluorescent staining for PPAR $\alpha$  (red) and SREBP1 (green) show that the Irbe (100  $\mu$ M) treatment increased the nuclear expression of the PPAR $\alpha$  protein while decreasing that of SREBP1. (B, C) Dual immunofluorescent staining for PPAR $\alpha$  (red) and p21 (B) or p27 (C) (green) showed that the Irbe treatment increased the expression of both proteins, and their distribution was almost consistent. \* $p < 0.05$ .

also reported in the intestines, pancreas, lungs, and placenta [36]. PPAR $\alpha$  in the human liver may effectively induce the expression of numerous genes involved in lipid, lipoprotein, and sugar metabolism [37]. However, the function of PPAR $\alpha$  in other PPAR $\alpha$ -expressing tissues, including the normal endometrium, has not yet been elucidated in detail. Recent studies revealed that PPAR $\alpha$  has anti-inflammatory [38,39] and anti-oxidant stress functions [40]. The normal endometrium exhibits high anti-inflammatory [39] and antioxidant activities to maintain fertility [41]. Further studies are needed to clarify the function of PPAR $\alpha$  in the normal endometrium.

The nuclear expression of PPAR $\alpha$  was lower in EMC cells than in the normal endometrium. In EMC, the expression of PPAR $\alpha$  was significantly lower in G3 than in G1. This result was inconsistent with previous findings [42,43], which showed stronger PPAR $\alpha$  staining in EMC tissues. In these studies, positive PPAR $\alpha$  staining was mainly observed in the cytoplasm and perinuclear area, and a detailed quantitative evaluation of nuclear PPAR $\alpha$  expression was not performed. Regarding colon cancer [44] and ampullary cancer [45], the expression of PPAR $\alpha$  was higher in cancer tissues than in their normal counterparts, which is inconsistent with the present pattern, whereas its expression was lower in mouse

lung cancer [46]. Therefore, the higher or lower expression of PPAR $\alpha$  in neoplastic tissues than in normal tissues may depend on the tissue context.

The immunohistochemical expression of SREBP1 and its target gene, FAS, was significantly higher in EMC than in normal endometrial glands, which was in contrast to that of PPAR $\alpha$ . This result is consistent with previous findings supporting the carcinogenic nature of SREBP1 [47]. Collectively, the results of immunostaining for PPAR $\alpha$  and SREBP1/FAS in normal and malignant endometrial tissues revealed an inverse correlation. Therefore, PPAR $\alpha$  may regulate tumor cell proliferation by interfering with the expression of SREBP1 and FAS.

The mechanisms underlying the down-regulation of PPAR $\alpha$  and up-regulation of SREBP1 in EMC tissues currently remain unclear. Several genetic changes in EMC, such as mutations in PTEN, PIK3CA, and microsatellite instability are reportedly involved in endometrial carcinogenesis [48,49]. However, a direct link between these mutations and the expression of PPAR $\alpha$ /SREBP1 has not yet been reported. An endocrinological environment may contribute to this result, i.e., a previous study reported that the expression of androgen receptor was higher in endometrial tissues than in the normal endometrium [50], while another study showed that serum levels of testosterone were higher in patients with EMC than in control women [51]. In addition, the prenatal exposure of fetal mice to testosterone resulted in the decreased expression of PPAR $\alpha$  in newborns. These findings may explain the reduced expression of PPAR $\alpha$  in EMC tissues.

In the present study, we used Irbe to activate PPAR $\alpha$  in EMC cells because it is superior to other peroxisome activators (fibrates) for organ damage [52,53]. To the best of our knowledge, this is the first study to examine the effects of Irbe on EMC cells. The results obtained revealed that Irbe increased the expression of PPAR $\alpha$  and suppressed the proliferation and migration of EMC, Ishikawa, and HEC1A cells. According to the PPAR $\alpha$  activation and silencing experiment in this study, the relationship between PPAR $\alpha$  and SREBP1/FAS was consistent with immunostaining. Previous studies showed that SREBP1 is an accelerating factor for the tumorigenesis of EMC [47]. Therefore, PPAR $\alpha$  may functionally inhibit the occurrence of EMC by inhibiting the SREBP1 pathway in the normal endometrium. In addition, the cell cycle regulators p21 and p27, which are closely related to tumor suppression, may participate in the suppression of EMC in association with PPAR $\alpha$ . The loss of PPAR $\alpha$  in the intestines has been proposed to increase DNMT1 (methyltransferase 1)-mediated p21 methylation and PRMT6 (protein arginine methyltransferase 6)-mediated p27 methylation, thereby promoting the development of colon cancer. In addition, an activator of PPAR $\alpha$  reduced the expression of DNMT1 and PRMT6 [23]. Therefore, PPAR $\alpha$  may play a role in EMC through the DNMT1/PRMT6-p21/p27 regulatory pathway. Another interesting result in the present study was that the expression of ARID1A, a key subunit of the SWI/SNF complex and a common tumor suppressor gene frequently mutated in gynecologic cancers [54,55], positively correlated

with the expression of PPAR $\alpha$ . A recent study reported that the antioxidant enzyme, SOD2, reduced the expression of the ARID1A gene [56]. In our experiments, the oxidative stress markers SOD2 and GPx1 were both affected by PPAR $\alpha$  gene silencing and the Irbe treatment, and this pattern was similar to that of ARID1A. Therefore, PPAR $\alpha$  may affect the expression of ARID1A by regulating oxidative stress. Collectively, these results suggest that the anti-tumor function of PPAR $\alpha$  involved not only SREBP1, but also p21/p27, antioxidant enzymes, and ARID1A.

In addition, Irbe has strong advantages for systemic use in EMC patients. EMC closely correlated with obesity and elevated serum TG levels [57,58]. Hypertriglyceridemia is a risk factor for EMC [59,60]. A previous study reported that fenofibrate, an activator of PPAR $\alpha$ , induced typical changes in serum lipids, including reductions in serum TG and increases in high-density lipoprotein cholesterol (HDL-c) [61]. Another study showed that the TG/HDL-c ratio may be a useful biological indicator for the treatment of EMC [62]. Moreover, PPAR $\alpha$  is closely related to obesity and insulin resistance [63–65]. Animal experiments revealed that PPAR $\alpha$  activators significantly attenuated type II insulin resistance [66,67]. Insulin resistance is an essential factor for metabolic syndrome and obesity-related carcinogenesis, including EMC [68–71]. In addition, a previous study demonstrated that the amount of insulin was higher in EMC patients than in a normal group [72]. Therefore, a reduction of PPAR $\alpha$  may cause insulin resistance and promote EMC.

In conclusion, the present study clearly showed that the expression of PPAR $\alpha$ , SREBP1, and FAS played important roles in the development of EMC, including the regulation of EMC cell proliferation and migration. In addition, the activation of PPAR $\alpha$  by Irbe may inhibit the proliferation of EMC cells by regulating SREBP1 and FAS, the tumor suppressor genes p21 and p27, and the ARID1A pathway mediated by oxidative stress. These results indicate the therapeutic potential of Irbe against EMC.

**Funding Statement:** This work was supported by JSPS KAKENHI Grant Number 18K09285.

**Author Contributions:** Yu LU: Conception, drafting, experiments, data analysis; Tsutomu MIYAMOTO: Corresponding author, funding, conception, data analysis, revision of the manuscript; Hodaka TAKEUCHI: Experiments, data analysis; Fumi TSUNODA: Experiments, data analysis; Naoki TANAKA: Conception, interpretation of results, supervision; Tanri SHIOZAWA: Interpretation of results, supervision, revision of the manuscript.

**Availability of Data and Materials:** The datasets generated and/or analyzed during the present study are available from the corresponding author upon reasonable request.

**Ethics Approval:** The present study was approved by the Ethics Committee of Shinshu University School of Medicine (approval number: 5222). In the present study, the requirement for informed consent was waived because we

had already obtained comprehensive consent to use removed tissue sections for any retrospective research from patients and allowed them to opt out of this study.

**Conflicts of Interest:** The authors declare that they have no conflicts of interest to report regarding the present study.

## References

- Malpica, A., Euscher Elizabeth, D., Hecht, J. L., Ali-Fehmi, R., Quick, C. M. et al. (2019). EMC, grossing and processing issues: Recommendations of the international society of gynecologic pathologists. *International Journal of Gynecological Pathology*, 38, S9–S24. <https://doi.org/10.1097/PGP.0000000000000552>
- Raglan, O., Kalliala, I., Markozannes, G., Cividini, S., Gunter, M. J. et al. (2019). Risk factors for endometrial cancer: An umbrella review of the literature. *International Journal of Cancer*, 145(7), 1719–1730. <https://doi.org/10.1002/ijc.31961>
- Pavlova, N. N., Thompson, C. B. (2016). The emerging hallmarks of cancer metabolism. *Cell Metabolism*, 23(1), 27–47. <https://doi.org/10.1016/j.cmet.2015.12.006>
- Sun, Y., Shi, Z., Lian, H., Cai, P. (2016). Energy metabolic dysfunction as a carcinogenic factor in cancer cells. *Clinical and Translational Medicine*, 5(1), 1–6. <https://doi.org/10.1186/s40169-016-0094-5>
- Wu, W., Zhao, S. (2013). Metabolic changes in cancer: Beyond the Warburg effect. *Acta Biochimica et Biophysica Sinica*, 45(1), 18–26.
- Anagnostou, E., Miliaras, D., Meditskou, S., Grimbizis, G. (2017). Immunohistochemical investigation of metabolic markers fatty acid synthase (FASN) and glucose transporter 1 (GLUT1) in normal endometrium, endometrial hyperplasia, and endometrial malignancy. *Hippokratia*, 21(4), 169–174.
- Goldstein, J. L., Brown, M. S. (2015). A century of cholesterol and coronaries: From plaques to genes to statins. *Cell*, 161(1), 161–172. <https://doi.org/10.1016/j.cell.2015.01.036>
- Goldstein, J. L., DeBose-Boyd, R. A., Brown, M. S. (2006). Protein sensors for membrane sterols. *Cell*, 124(1), 35–46. <https://doi.org/10.1016/j.cell.2005.12.022>
- Nohturfft, A., Zhang, S. C. (2009). Coordination of lipid metabolism in membrane biogenesis. *Annual Review of Cell and Developmental Biology*, 25(1), 539–566. <https://doi.org/10.1146/annurev.cellbio.24.110707.175344>
- Li, J. N., Mahmoud, M. A., Han, W. F., Ripple, M., Pizer, E. S. et al. (2000). Sterol regulatory element-binding protein-1 participates in the regulation of fatty acid synthase expression in colorectal neoplasia. *Experimental Cell Research*, 261(1), 159–165. <https://doi.org/10.1006/excr.2000.5054>
- Gao, Y., Nan, X., Shi, X., Mu, X., Liu, B. et al. (2019). SREBP1 promotes the invasion of colorectal cancer accompanied upregulation of MMP7 expression and NF- $\kappa$ B pathway activation. *BMC Cancer*, 19(1), 685–692. <https://doi.org/10.1186/s12885-019-5904-x>
- Yang, Y., Morin, P. J., Han, W., Chen, T., Bornman, D. M. et al. (2003). Regulation of fatty acid synthase expression in breast cancer by sterol regulatory element binding protein-1c. *Experimental Cell Research*, 282(2), 132–137. [https://doi.org/10.1016/S0014-4827\(02\)00023-X](https://doi.org/10.1016/S0014-4827(02)00023-X)
- Li, L., Hua, L., Fan, H., He, Y., Xu, W. et al. (2019). Interplay of PKD3 with SREBP1 promotes cell growth via upregulating lipogenesis in prostate cancer cells. *Journal of Cancer*, 10(25), 6395–6404. <https://doi.org/10.7150/jca.31254>
- Yahagi, N., Shimano, H., Hasegawa, K., Ohashi, K., Matsuzaka, T. et al. (2005). Co-ordinate activation of lipogenic enzymes in hepatocellular carcinoma. *European Journal of Cancer*, 41(9), 1316–1322. <https://doi.org/10.1016/j.ejca.2004.12.037>
- Escher, P., Wahli, W. (2000). Peroxisome proliferator-activated receptors: Insight into multiple cellular functions. *Mutation Research*, 448(2), 121–138. [https://doi.org/10.1016/S0027-5107\(99\)00231-6](https://doi.org/10.1016/S0027-5107(99)00231-6)
- Auboeuf, D., Rieusset, J., Fajas, L., Vallier, P., Frering, V. et al. (1997). Tissue distribution and quantification of the expression of mRNAs of peroxisome proliferator-activated receptors and liver X receptor-alpha in humans: No alteration in adipose tissue of obese and NIDDM patients. *Diabetes*, 6(8), 1319–1327. <https://doi.org/10.2337/diabetes.46.8.1319>
- Braissant, O., Foufelle, F., Scotto, C., Dauca, M., Wahli, W. et al. (1996). Differential expression of peroxisome proliferator-activated receptors (PPARs): Tissue distribution of PPAR-alpha, -beta, and -gamma in the adult rat. *Endocrinology*, 137(1), 354–366. <https://doi.org/10.1210/endo.137.1.8536636>
- Lu, Y., Harada, M., Kamijo, Y., Nakajima, T., Tanaka, N. et al. (2019). Peroxisome proliferator-activated receptor  $\alpha$  attenuates high-cholesterol diet-induced toxicity and pro-thrombotic effects in mice. *Archives of Toxicology*, 93(1), 149–161. <https://doi.org/10.1007/s00204-018-2335-4>
- Holland, C. M., Saidi, S. A., Evans, A. L., Sharkey, A. M., Latimer, J. A. et al. (2004). Transcriptome analysis of endometrial cancer identifies peroxisome proliferator-activated receptors as potential therapeutic targets. *Molecular Cancer Therapeutics*, 3(8), 993–1001. <https://doi.org/10.1158/1535-7163.993.3.8>
- Yoshikawa, T., Ide, T., Shimano, H., Yahagi, N., Amemiya-Kudo, M. et al. (2003). Cross-talk between peroxisome proliferator activated receptor (PPAR) and liver X receptor (LXR) in nutritional regulation of fatty acid metabolism. I. PPARs suppress sterol regulatory element binding protein-1c promoter through inhibition of LXR signaling. *Molecular Endocrinology*, 17(7), 1240–1254. <https://doi.org/10.1210/me.2002-0190>
- König, B., Koch, A., Spielmann, J., Hilgenfeld, C., Hirche, F. et al. (2009). Activation of PPARalpha and PPARgamma reduces triacylglycerol synthesis in rat hepatoma cells by reduction of nuclear SREBP-1. *European Journal of Pharmacology*, 605(1–3), 23–30. <https://doi.org/10.1016/j.ejphar.2009.01.009>
- Mitrea, D. M., Yoon, M. K., Ou, L., Kriwacki, R. W. (2012). Disorder-function relationships for the cell cycle regulatory proteins p21 and p27. *Biological Chemistry*, 393(4), 159–274. <https://doi.org/10.1515/hsz-2011-0254>
- Luo, Y., Xie, C., Brocker, C. N., Fan, J., Wu, X. et al. (2019). Intestinal PPAR $\alpha$  protects against colon carcinogenesis via regulation of methyltransferases DNMT1 and PRMT6. *Gastroenterology*, 157(3), 744–759. <https://doi.org/10.1053/j.gastro.2019.05.057>
- Guan, B., Mao, T. L., Panuganti, P. K., Kuhn, E., Kurman, R. J. et al. (2011). Mutation and loss of expression of ARID1A in uterine low-grade endometrioid carcinoma. *American Journal of Surgical Pathology*, 35(5), 625–632. <https://doi.org/10.1097/PAS.0b013e318212782a>
- Rong, X., Li, Y., Ebihara, K., Zhao, M., Kusakabe, T. et al. (2010). Irbesartan treatment up-regulates hepatic expression of PPARalpha and its target genes in obese Koletsky ( $fa^k/fa^k$ ) rats: A link to amelioration of hypertriglyceridaemia. *British Journal of Pharmacology*, 160(7), 1796–1807. <https://doi.org/10.1111/j.1476-5381.2010.00835.x>

26. Nowakowska, M., Matysiak-Burzyńska, Z., Kowalska, K., Elżbieta, P., Domińska, K. et al. (2016). Angiotensin II promotes endometrial cancer cell survival. *Oncology Reports*, 36(2), 1101–1110. <https://doi.org/10.3892/or.2016.4887>
27. Ida, K., Yamanoi, K., Asaka, S., Takeuchi, H., Miyamoto, T. et al. (2019).  $\alpha$ GlcNAc and its catalyst  $\alpha$ 4GnT are diagnostic and prognostic markers in uterine cervical tumor, gastric type. *Scientific Reports*, 9(1), 13043. <https://doi.org/10.1038/s41598-019-49376-7>
28. Ando, H., Miyamoto, T., Kashima, H., Higuchi, S., Ida, K. et al. (2017). Panobinostat enhances growth suppressive effects of progestin on endometrial carcinoma by increasing progesterone receptor and mitogen-inducible gene-6. *Hormones & Cancer*, 8(4), 257–267. <https://doi.org/10.1007/s12672-017-0295-4>
29. Ko, C., Park, W. J., Park, S., Kim, S., Windisch, M. P. et al. (2015). The FDA-approved drug irbesartan inhibits HBV-infection in HepG2 cells stably expressing sodium taurocholate co-transporting polypeptide. *Antiviral Therapy*, 20(8), 835–842. <https://doi.org/10.3851/IMP2965>
30. Miyamoto, T., Kashima, H., Yamada, Y., Kobara, H., Asaka, R. et al. (2016). Lipocalin 2 enhances migration and resistance against cisplatin in endometrial carcinoma cells. *PLoS One*, 11(5), e0155220. <https://doi.org/10.1371/journal.pone.0155220>
31. Higuchi, S., Miyamoto, T., Kobara, H., Yamada, S., Asaka, R. et al. (2019). Trophoblast type-specific expression of senescence markers in the human placenta. *Placenta*, 85, 56–62. <https://doi.org/10.1016/j.placenta.2019.06.377>
32. Yellaturu, C. R., Deng, X., Cagen, L. M., Wilcox, H. G., Mansbach II, C. M. et al. (2009). Insulin enhances post-translational processing of nascent SREBP-1c by promoting its phosphorylation and association with COPII vesicles. *Journal of Biological Chemistry*, 284(12), 7518–7532. <https://doi.org/10.1074/jbc.M805746200>
33. Han, J., Li, E., Chen, L., Zhang, Y., Wei, F. et al. (2015). The CREB coactivator CRTC2 controls hepatic lipid metabolism by regulating SREBP1. *Nature*, 524(7564), 243–256. <https://doi.org/10.1038/nature14557>
34. Klaunig, J. E. (2018). Oxidative stress and cancer. *Current Pharmaceutical Design*, 24(40), 4771–4778. <https://doi.org/10.2174/1381612825666190215121712>
35. Lee, S. S., Pineau, T., Drago, J., Lee, E. J., Owens, J. W. et al. (1995). Targeted disruption of the alpha isoform of the peroxisome proliferator-activated receptor gene in mice results in abolishment of the pleiotropic effects of peroxisome proliferators. *Molecular and Cellular Biology*, 15(6), 3012–3022. <https://doi.org/10.1128/MCB.15.6.3012>
36. Kersten, S., Stienstra, R. (2017). The role and regulation of the peroxisome proliferator activated receptor alpha in human liver. *Biochimie*, 136, 75–84. <https://doi.org/10.1016/j.biochi.2016.12.019>
37. Shirinsky, I. V., Shirinsky, V. S. (2011). Targeting nuclear hormone receptors: PPAR $\alpha$  agonists as potential disease-modifying drugs for rheumatoid arthritis. *International Journal of Rheumatology*, 2011(2), 937843. <https://doi.org/10.1155/2011/937843>
38. Muzio, G., Barrera, G., Pizzimenti, S. (2021). Peroxisome proliferator-activated receptors (PPARs) and oxidative stress in physiological conditions and in cancer. *Antioxidants*, 10(11), 1734. <https://doi.org/10.3390/antiox10111734>
39. Sekulic-Jablanovic, M., Petkovic, V., Wright, M. B., Kucharava, K., Huerzeler, N. et al. (2017). Effects of peroxisome proliferator activated receptors(PPAR)- $\gamma$  and - $\alpha$  agonists on cochlear protection from oxidative stress. *PLoS One*, 12(11), 1–19.
40. Kunicka, Z., Kurzyńska, A., Szydłowska, A., Bogacka, I. (2020). Peroxisome proliferator-activated receptor alpha regulates the expression of the immune response mediators in the porcine endometrium during the estrous cycle and early pregnancy. *American Journal of Reproductive Immunology*, 83(3), e13211. <https://doi.org/10.1111/aji.13211>
41. Sugino, N., Shimamura, K., Takiguchi, S., Tamura, H., Ono, M. et al. (1996). Changes in activity of superoxide dismutase in the human endometrium throughout the menstrual cycle and in early pregnancy. *Human Reproduction*, 11(5), 1073–1078. <https://doi.org/10.1093/oxfordjournals.humrep.a019299>
42. Knapp, P., Chabowski, A., Błachnio-Zabielska, A., Jarzabek, K., Wolczyński, S. (2012). Altered peroxisome-proliferator activated receptors expression in human endometrial cancer. *PPAR Research*, 2012(1), 471524. <https://doi.org/10.1155/2012/471524>
43. Nickkho-Amiry, M., McVey, R., Holland, C. (2012). Peroxisome-proliferator activated receptors modulate proliferation and angiogenesis in human endometrial carcinoma. *Molecular Cancer Research*, 10(3), 411–453. <https://doi.org/10.1158/1541-7786.MCR-11-0233>
44. Morinishi, T., Tokuhara, Y., Ohsaki, H., Ibuki, E., Kadota, K. et al. (2019). Activation and expression of peroxisome proliferator-activated receptor alpha are associated with tumorigenesis in colorectal carcinoma. *PPAR Research*, 2019(3), 7486727. <https://doi.org/10.1155/2019/7486727>
45. Wang, C. Y., Chao, Y. J., Chen, Y. L., Wang, T. W., Phan, N. N. et al. (2021). Upregulation of peroxisome proliferator-activated receptor- $\alpha$  and the lipid metabolism pathway promotes carcinogenesis of ampullary cancer. *International Journal of Medical Science*, 18(1), 256–269. <https://doi.org/10.7150/ijms.48123>
46. Li, X., Lu, Y., Ou, X., Zeng, S., Wang, Y. et al. (2020). Changes and sex- and age-related differences in the expression of drug metabolizing enzymes in a KRAS-mutant mouse model of lung cancer. *PeerJ*, 8(12), e10182. <https://doi.org/10.7717/peerj.10182>
47. Li, W., Tai, Y., Zhou, J., Gu, W., Bai, Z. et al. (2012). Repression of endometrial tumor growth by targeting SREBP1 and lipogenesis. *Cell Cycle*, 11(12), 2348–2358. <https://doi.org/10.4161/cc.20811>
48. Banno, K., Yanokura, M., Iida, M., Masuda, K., Aoki, D. (2014). Carcinogenic mechanisms of endometrial cancer: Involvement of genetics and epigenetics. *Journal of Obstetrics and Gynaecology Research*, 40(8), 1957–1967. <https://doi.org/10.1111/jog.12442>
49. Robertson, A. G., Pashtan, I., Shen, R., Benz, C. C., Yau, C. et al. (2013). Integrated genomic characterization of endometrial carcinoma. *Nature*, 497(7447), 67–73. <https://doi.org/10.1038/nature12113>
50. Tangen, I. L., Onyango, T. B., Kopperud, R., Berg, A., Halle, M. K. et al. (2018). Androgen receptor as potential therapeutic target in metastatic endometrial cancer. *Oncotarget*, 14(6), 1011–1027.
51. Audet-Walsh, E., Lépine, J., Grégoire, J., Plante, M., Caron, P. et al. (2011). Profiling of endogenous estrogens, their precursors, and metabolites in endometrial cancer patients: Association with risk and relationship to clinical

- characteristics. *Journal of Clinical Endocrinology and Metabolism*, 96(2), E330–E339. <https://doi.org/10.1210/jc.2010-2050>
52. Croom, K. F., Curran, M. P., Goa, K. L., Perry, C. M. (2004). Irbesartan a review of its use in hypertension and in the management of diabetic nephropathy. *Drugs*, 64(9).
  53. Jun, M., Zhu, B., Tonelli, M., Jardine, M. J., Patel, A. et al. (2012). Effects of fibrates in kidney disease. *Journal of the American College of Cardiology*, 60(20), 2061–2071. <https://doi.org/10.1016/j.jacc.2012.07.049>
  54. Wiegand, K. C., Shah, S. P., Al-Agha, O. M., Zhao, Y., Tse, K. et al. (2010). ARID1A mutations in endometriosis-associated ovarian carcinomas. *New England Journal of Medicine*, 363(16), 1532–1543. <https://doi.org/10.1056/NEJMoa1008433>
  55. Jones, S., Wang, T. L., Shih, I. M., Mao, T. L., Nakayama, K. et al. (2010). Frequent mutations of chromatin remodeling gene ARID1A in ovarian clear cell carcinoma. *Science*, 330(6001), 228–231. <https://doi.org/10.1126/science.1196333>
  56. Winarto, H., Tan, M. I., Sadikin, M., Wanandi, S. I. (2017). ARID1A expression is down-regulated by oxidative stress in endometriosis and endometriosis associated ovarian cancer. *Translational Oncogenomics*, 9, 1177272716689818. <https://doi.org/10.1177/1177272716689818>
  57. Ulmer, H., Borena, W., Rapp, K., Klenk, J., Strasak, A. (2009). Serum triglyceride concentrations and cancer risk in a large cohort study in Austria. *British Journal of Cancer*, 101(7), 1202–1206. <https://doi.org/10.1038/sj.bjc.6605264>
  58. Lindemann, K., Vatten, L. J., Ellström-Eng, M., Eskild, A. (2009). Serum lipids and endometrial cancer risk: Results from the HUNT-II study. *International Journal of Cancer*, 124(12), 2938–2941. <https://doi.org/10.1002/ijc.24285>
  59. Eckel, R. H., Grundy, S. M., Zimmet, P. Z. (2008). The metabolic syndrome. *Endocrine Reviews*, 29(7), 777–822. <https://doi.org/10.1210/er.2008-0024>
  60. Rosato, V., Zucchetto, A., Bosetti, C., Maso, L. D., Montella, M. (2011). Metabolic syndrome and endometrial cancer risk. *Annals of Oncology*, 22(4), 884–889. <https://doi.org/10.1093/annonc/mdq464>
  61. Kraja, A. T., Province, M. A., Straka, R. J., Ordovas, J. M., Borecki, I. B. et al. (2010). Fenofibrate and metabolic syndrome. *Endocrine Metabolic and Immune Disorders Drug Targets*, 10(2), 138–148. <https://doi.org/10.2174/187153010791213047>
  62. Luo, Y. Z., Yang, Z., Qiu, Y. L., Li, X. H., Qin, L. Q. et al. (2019). Pretreatment triglycerides-to-high density lipoprotein cholesterol ratio in postmenopausal women with endometrial cancer. *Kaohsiung Journal of Medical Sciences*, 35(5), 303–309. <https://doi.org/10.1002/kjm2.12033>
  63. Haluzik, M. M., Haluzik, M. (2006). Peroxisome proliferator activated receptors (PPAR) and insulin sensitivity: Experimental studies. *Ceskoslovenská Fysiologie*, 55(4), 163–168.
  64. Anderlová, K., Dolezalová, R., Housová, J., Bosanská, L., Haluziková, D. et al. (2007). Influence of PPAR- $\alpha$  agonist fenofibrate on insulin sensitivity and selected adipose tissue-derived hormones in obese women with type 2 diabetes. *Physiological Research*, 56, 579–586.
  65. Haluzik, M. M., Haluzik, M. (2006). PPAR- $\alpha$  and insulin sensitivity. *Physiological Research*, 55, 115–122.
  66. Koh, E. H., Kim, M. S., Park, J. Y., Kim, H. S., Youn, J. et al. (2003). Peroxisome proliferator-activated receptor (PPAR)- $\alpha$  activation prevents diabetes in OLETF rats comparison with PPAR- $\gamma$  activation. *Diabetes*, 52(9), 2331–2337. <https://doi.org/10.2337/diabetes.52.9.2331>
  67. Tsunoda, M., Kobayashi, N., Ide, T., Utsumi, M., Nagasawa, M. et al. (2008). A novel PPAR $\alpha$  agonist ameliorates insulin resistance in dogs fed a high-fat diet. *American Journal of Physiology Endocrinology and Metabolism*, 294(5), 833–840. <https://doi.org/10.1152/ajpendo.00627.2007>
  68. Linkov, F., Goughnour, S. L., Ma, T., Xu, Z., Edwards, R. et al. (2017). Changes in inflammatory endometrial cancer risk biomarkers in individuals undergoing surgical weight loss. *Gynecologic Oncology*, 147(1), 133–1338. <https://doi.org/10.1016/j.ygyno.2017.07.144>
  69. Liao, C., Zhang, D., Mungo, C., Tompkins, D. A., Zeidan, A. M. (2014). Is diabetes mellitus associated with increased incidence and disease-specific mortality in endometrial cancer? A systematic review and meta-analysis of cohort studies. *Gynecologic Oncology*, 135(1), 163–171. <https://doi.org/10.1016/j.ygyno.2014.07.095>
  70. Zhang, Y., Liu, H., Yang, S., Zhang, J., Qian, L. et al. (2014). Overweight, obesity and endometrial cancer risk: results from a systematic review and meta-analysis. *The International Biological Markers*, 29(1), 21–29. <https://doi.org/10.5301/IBM.5000047>
  71. Zhang, Z. H., Su, P. Y., Hao, J. H., Sun, Y. H. (2013). The role of preexisting diabetes mellitus on incidence and mortality of endometrial cancer: A meta-analysis of prospective cohort studies. *International Journal of Gynecological Cancer*, 23(2), 294–303. <https://doi.org/10.1097/IGC.0b013e31827b8430>
  72. Wang, Y., Hua, S., Tian, W., Zhang, L., Zhao, J. et al. (2012). Mitogenic and anti-apoptotic effects of insulin in endometrial cancer are phosphatidylinositol 3-kinase/Akt dependent. *Gynecologic Oncology*, 125(3), 734–741. <https://doi.org/10.1016/j.ygyno.2012.03.012>

## Supplementary Materials

TABLE S1

## Primer sequences

Gene name	Primer name	Sequence
PPAR $\alpha$	PPAR $\alpha$ -F	CGTCCTGGCCTTCTAAACGT
	PPAR $\alpha$ -R	GCATCCGACTCCGTCTTCTT
SREBP1	SREBP1-F	GATGCGGAGAAGCTGCCTAT
	SREBP1-R	TTGCGCAAGACAGCAGATTT
FAS	FAS-F	TGCGTGGCCTTTGAAATGTG
	FAS-R	CTCCATGTCCGTGAACTGCT
p21(CDKN1A)	p21-F	ATGTGCACGGAAGGACTTTGT
	p21-R	ATGTAGAGCGGGCCTTTGAG
p27(CDKN1B)	p27-F	GGGGTCTGTGTCTTTTGGCT
	p27-R	AGACACTCGCACGTTTGACA
SOD1	SOD1-F	AAAGATGGTGTGGCCGATGT
	SOD1-R	CAAGCCAAACGACTTCCAGC
SOD2	SOD2-F	GCCTACGTGAACAACCTGAAC
	SOD2-R	TGGAATAAGGCCTTTGGGTTCT
GPX1	GPX1-F	AGTCGGTGTATGCCTTCTCG
	GPX1-R	TCTTGGCGTTCTCCTGATGC
NQO1	NQO1-F	CCTTGTGATATCCAGAGTGGC
	NQO1-R	AAGAGGCTGCTTGGAGCAAA
ARID1A	ARID1A-F	TCATGCCTTCCAACCCAGAC
	ARID1A-R	GCTGGATACCTGCTGTTGCT
ACTB	ACTB-F	GACAGGATGCAGAAGGAGATTACT
	ACTB-R	TGATCCACATCTGCTGGAAGGT

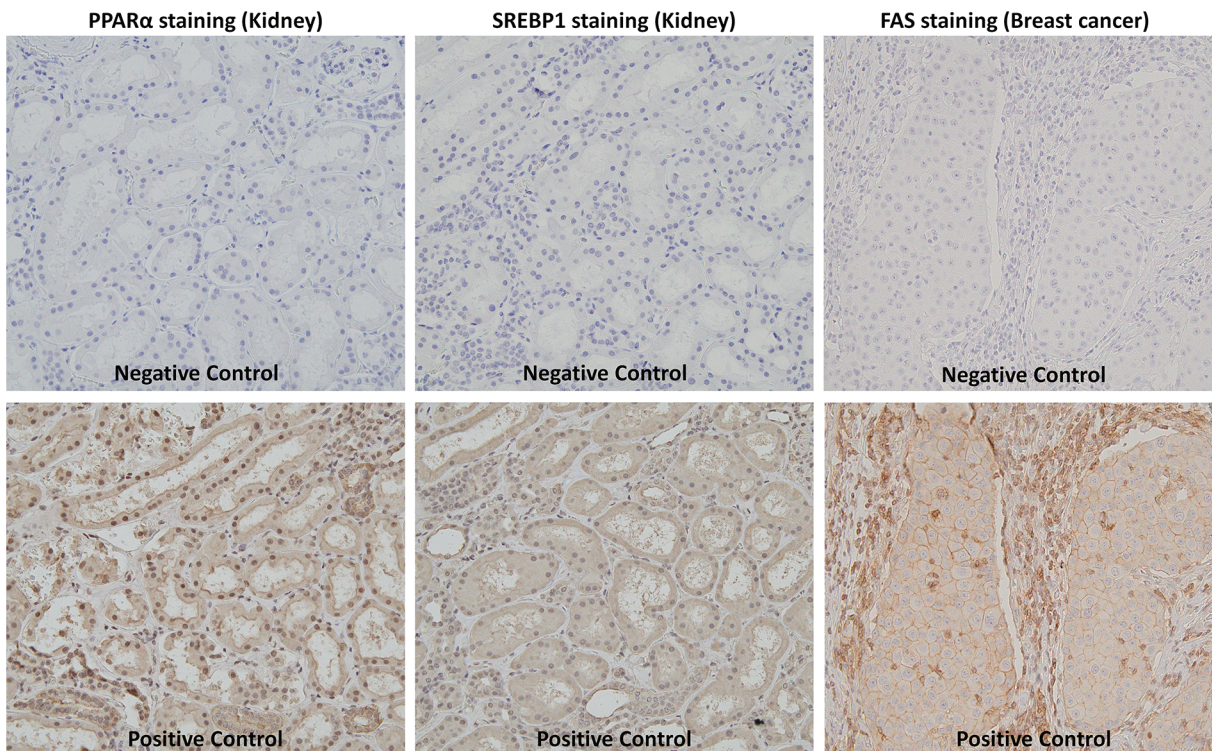
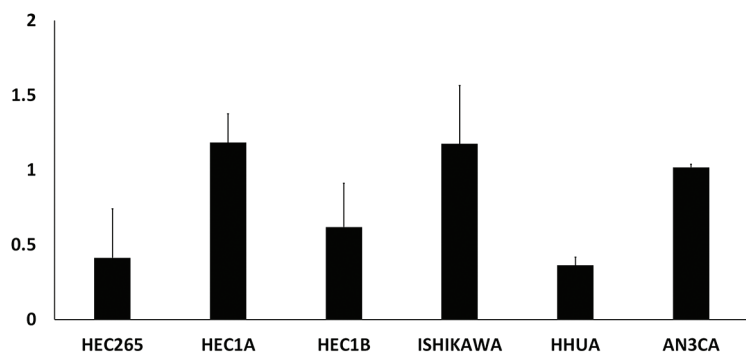


FIGURE S1. Negative and positive control of immunostaining.



**FIGURE S2.** Relative expression of PPAR $\alpha$  mRNA in EMC cell lines.